Thermally stimulated currents due to multiple-trapping carrier transport. II. Dispersive transport

1992 J. Phys.: Condens. Matter 4 3985

(http://iopscience.iop.org/0953-8984/4/15/013)

J. Phys.: Condens. Matter 4 (1992) 3985–4002. Printed in the UK

Thermally stimulated currents due to multiple-trapping carrier transport: II. Dispersive transport

W Tomaszewicz
Laboratory of Organic Dielectrics and Semiconductors, Technical University of Gdańsk, Majakowskiego 11/12, 80-952 Gdańsk, Poland

Received 4 November 1991

Abstract. This paper deals with non-isothermal dispersive carrier transport in an insulator with trapping states. The approximate solutions of the transport equations derived previously are extended here to include an arbitrary spatial distribution of generated carriers as well as the temperature and energy dependences of some trap parameters and the temperature dependence of the microscopic carrier mobility. The accuracy of the formulae describing thermally stimulated currents (TSC) is verified by Monte Carlo calculations for exponential and Gaussian trap distributions. Methods of determining the shape of the trap distribution and the trap parameters from the TSC data are discussed.

1. Introduction

A major advance in understanding the electronic transport properties of disordered solids was the development of the theory of dispersive carrier transport by Scher and Montroll [1], Noolandi [2, 3], Schmidlin [4] and other authors (see reviews [5, 6]). They explained satisfactorily the extremely large dispersion of the transit times of excess carriers, revealed in the time-of-flight (TOF) measurements for many disordered materials. It was recognized that dispersive transport is related to the non-equilibrium occupancy of the localized states, for both trap-controlled and hopping transport mechanisms.

In the 1980s, the mentioned theory was extended to the case of non-isothermal carrier transport [7–11], thus giving a new theory of thermally stimulated currents (TSC). Except for variable sample temperature, the assumptions of the 'TSC drift experiment' follow closely those of the TOF method. It was presupposed that the excess carriers are initially generated in the surface layer of the sample by light or ionizing radiation. Next, the sample is heated gradually, and the TSC induced by carrier drift in the applied field is monitored. It was shown that the described TSC technique can yield the same information about the localized states in the solid as the most commonly used TOF method.

Regarding the TSC caused by dispersive multiple-trapping carrier transport, two main approaches have been put forward by Plans *et al* [8] and Tomaszewicz and Jachym [10]. Both works were based on the simplified theory of isothermal dispersive transport [12–14] and gave similar results, despite the somewhat different approximations used for solving the transport equations. In this paper, the results obtained in [10] are extended

0953-8984/92/153985 + 18 $04.50

to cover the cases of arbitrary spatial distribution of the generated carriers, as well as of temperature-dependent microscopic carrier mobility and some temperature- and energy-dependent trap parameters. The accuracy of the formulae describing TSC is proved by Monte Carlo calculations for model trap distributions. A more extensive review of the literature, as well as more details concerning the formulation of the transport equations and the Monte Carlo method, are given in the preceding paper (hereafter referred to as I) dealing with non-dispersive TSC.

2. Formulation of the problem

2.1. Transport equations

The equations describing non-isothermal carrier transport in a solid with trapping states are derived in section 2.2 of I. Only the equations themselves are repeated here for convenience:

$$\partial[n(z,t)+n_t(z,t)]/\partial t + u(t)\,\partial n(z,t)/\partial z = 0 \tag{1}$$

$$n_t(z,t) = \int_0^t \Phi(t,t')n(z,t')\,dt' \qquad t \geqslant 0 \tag{2}$$

$$\Phi(t,t') = \int_{\varepsilon_t^0}^{\varepsilon_t} C_t(\varepsilon,t')N_t(\varepsilon)\exp\left(-\int_{t'}^{t}\frac{dt''}{\tau_r(\varepsilon,t'')}\right)d\varepsilon \tag{3}$$

$$\tau_r(\varepsilon,t) = \nu^{-1}(\varepsilon,t)\exp[\varepsilon/kT(t)] \tag{4}$$

$$I(t) = \frac{I_0 u(t)}{n_0 \tau_0}\int_0^{\tau_0} n(z,t)\,dz. \tag{5}$$

2.2. Dispersive transport regime

Dispersive transport is characterized by a progressive thermalization of the carriers with trapping states distributed in a wide energy region, $\varepsilon_t - \varepsilon_t^0 \gg kT(t)$. In the following, we shall assume that the function $C_t(\varepsilon,t)N_t(\varepsilon)$ varies slowly with energy compared to the Boltzmann factor $\exp[\varepsilon/kT(t)]$. The dominant part of the carriers then occupies relatively deep traps, from which no carrier emission takes place up to the given time t. Since the probability of carrier emission from these traps does not depend on the moment t' of carrier capture, formula (3) for $\Phi(t,t')$ can be simplified by setting $t'=0$ in the lower limit of the integral in the exponential factor (cf. [10]). Furthermore, we assume that the functions $C_t(\varepsilon,t)$ and—as implied by the detailed equilibrium principle (I, equation (5))—$\nu(\varepsilon,t)$ can be expressed in the factorized form:

$$C_t(\varepsilon,t) = w(t)C_{t0}(\varepsilon) \tag{6}$$

$$\nu(\varepsilon,t) = w(t)[T(t)/T_0]^{3/2}\nu_0(\varepsilon) \tag{7}$$

where $C_{t0}(\varepsilon) = C_t(\varepsilon,0)$, $\nu_0(\varepsilon) = \nu(\varepsilon,0)$ and the initial sample temperature $T_0 = T(0)$. This assumption is unnecessary if $C_t(\varepsilon,t)$ and $\nu(\varepsilon,t)$ depend solely on one variable, ε or t. The function $\Phi(t,t')$ then takes the form

$$\Phi(t,t') = w(t')\Phi(t,0) \tag{8}$$

where

$$\Phi(t,0)=\int_{\varepsilon_t^0}^{\varepsilon_t} C_{t0}(\varepsilon)N_t(\varepsilon)\exp\left(-\int_0^t \frac{dt'}{\tau_r(\varepsilon,t')}\right)d\varepsilon. \tag{9}$$

One can note that equation (8) is also valid for the initial stage of carrier transport. In such a case carrier detrapping and the time variation of the carrier trapping probability are negligible, which implies that $\Phi(t,t')\simeq\Phi(t,0)\simeq 1/\tau_{t0}$, where τ_{t0} is the mean free-carrier lifetime at the initial moment (cf. I, equation (16)). In the last formula the exponential term in the integrand may be approximated by the unit step function $H[\varepsilon-\varepsilon_0(t)]$, where the demarcation level $\varepsilon_0(t)$ is given by the implicit equation [8, 10]

$$\int_0^t \frac{dt'}{\tau_r[\varepsilon_0(t),t']}=1. \tag{10}$$

This yields the simple formula

$$\Phi(t,0)\simeq\int_{\varepsilon_0(t)}^{\varepsilon_t} C_{t0}(\varepsilon)N_t(\varepsilon)\,d\varepsilon \tag{11}$$

valid for $\varepsilon_t^0<\varepsilon_0(t)<\varepsilon_t$. The level $\varepsilon_0(t)$ separates the shallower traps, which reached equilibrium occupancy, and the deeper ones, characterized by non-equilibrium population. Dispersive transport occurs therefore in the time region given implicitly by the above inequality.

By inserting formula (8) into equation (2) we obtain, after simple transformations, the approximate equation describing the trapping/detrapping kinetics for dispersive transport:

$$\frac{\partial}{\partial t}\left(\frac{n_t(z,t)}{\Phi(t)}\right)\simeq w(t)n(z,t) \tag{12}$$

where $\Phi(t)\equiv\Phi(t,0)$. The physical meaning of the above equation may be better understood after its rearrangement into the form

$$\frac{\partial n_t(z,t)}{\partial t}\simeq w(t)\Phi(t)n(z,t)+\frac{1}{\Phi(t)}\frac{d\Phi(t)}{dt}n_t(z,t). \tag{13}$$

One can show that the first and second terms on the RHS represent, respectively, the rates of carrier capture in the energy region $\varepsilon\geqslant\varepsilon_0(t)$, and of carrier emission from traps of depth equal to $\varepsilon_0(t)$ (cf. [10]). In the above approximation the processes of carrier trapping and detrapping in the energy range $\varepsilon<\varepsilon_0(t)$ are ignored.

To simplify the transport equations further, we omit the term $\partial n(z,t)/\partial t$ from the continuity equation (1), which yields

$$\partial n_t(z,t)/\partial t+u(t)\,\partial n(z,t)/\partial z\simeq 0. \tag{14}$$

In the case of temperature-independent parameters $\mu_0(t)$ and $C_{t0}(\varepsilon,t)$ this approximation is valid for the time $t\gg z$ (cf. [10]). One may expect that the analogous criterion holds also in the present case. In the TSC experiments the measurement time $t\gg\tau_0\geqslant z$ and the considered approximation seems to be legitimate. In the following we assume that the carriers are generated in the sample by a light pulse of very short duration and

that no carrier injection takes place from the front electrode. Then the boundary condition for equations (12) and (14) is

$$n(0, t) = 0 \qquad t > 0. \tag{15}$$

In contrast to previous papers on the subject, we shall consider here the case of arbitrary initial distribution $n(z, 0)$ of carriers in the sample. However, the initial condition cannot be directly applied to equations (12) and (14), because the second of them is not valid for $t \ll z$. Instead, we assume that carrier detrapping and the time variation of $\mu(t)$ and $C_t(\varepsilon, t)$ are negligible in some time region from $t = 0$ to $t \gg z$. The corresponding solutions of exact transport equations (1)–(3) are (see appendix 1):

$$n(z, t) = 0 \tag{16}$$

$$n_t(z, t) = \frac{1}{\tau_{t0}} \int_0^z n(z', 0) \exp[-(z - z')/\tau_{t0}] \, dz' \tag{17}$$

where $t > z$. These expressions may be utilized as the initial conditions for equations (12) and (14). It should be mentioned that the applicability of the resulting formulae for TSC in the case of bulk carrier generation requires, contrary to the case of surface generation, negligible carrier recombination during the whole TSC run.

3. Analytical results

3.1. Solutions of transport equations

The system of equations (12) and (14) governing carrier transport does not seem to have solutions in terms of elementary functions. In the following, we shall confine ourselves to some cases that allow us to derive simple formulae describing TSC.

First, we shall neglect the temperature dependence of $\mu(t)$, $C_t(\varepsilon, t)$ and $\nu(\varepsilon, t)$, setting $u(t) = 1$ and $w(t) = 1$ in equations (5), (12) and (14). Equations (12) and (14) are then solved easily, and the general solutions fulfilling condition (15) are:

$$n(z, t) = \frac{\partial}{\partial t} \int_0^z g(z') \exp[-(z - z')\Phi(t)] \, dz' \tag{18}$$

$$n_t(z, t) = \Phi(t) \int_0^z g(z') \exp[-(z - z')\Phi(t)] \, dz'. \tag{19}$$

The function $g(z)$ can be determined from conditions (16) and (17). Since in the case of no carrier retrapping $\Phi(t) = 1/\tau_{t0}$ (cf. preceding section), it is seen that $g(z) = n(z, 0)$. Inserting the free-carrier density (18) into equation (5), one obtains after simple transformations the following formula for TSC:

$$I(t) = I_0 \frac{d}{dt} \left[\frac{1}{\Phi(t)} \left(1 - \frac{1}{n_0 \tau_0} \int_0^{\tau_0} n(z, 0) \exp[-(\tau_0 - z)\Phi(t)] \, dz \right) \right]. \tag{20}$$

For surface carrier generation, corresponding to the initial condition

$$n(z, 0) = n_0 \tau_0 \delta(z) \tag{21}$$

from equation (20) one gets

$$I(t) = I_0 \frac{\mathrm{d}}{\mathrm{d}t}\left(\frac{1 - \exp[-\tau_0 \Phi(t)]}{\Phi(t)}\right). \tag{22}$$

This formula has already been derived in a somewhat different way in [10]. For uniform bulk carrier generation, when

$$n(z, 0) = n_0 \tag{23}$$

one obtains

$$I(t) = I_0 \frac{\mathrm{d}}{\mathrm{d}t}\left(\frac{\tau_0 \Phi(t) + \exp[-\tau_0 \Phi(t)] - 1}{\tau_0 \Phi^2(t)}\right). \tag{24}$$

We shall consider some general features of the TSC, given by equation (20). Provided that $\tau_0 \Phi(t) \gg 1$, the second term in the inner brackets can be neglected. Then, one obtains

$$I(t) \simeq I_0 \frac{\mathrm{d}}{\mathrm{d}t}\left(\frac{1}{\Phi(t)}\right). \tag{25}$$

On the other hand, if $\tau_0 \Phi(t) \ll 1$, the exponential function in the integrand in equation (20) may be expanded into a power series. Taking three initial terms, one gets

$$I(t) \simeq c I_0 \tau_0^2 [-\mathrm{d}\Phi(t)/\mathrm{d}t] \tag{26}$$

where the constant c is given by

$$c = \frac{1}{2 n_0 \tau_0} \int_0^{\tau_0} (1 - z/\tau_0)^2 n(z, 0)\, \mathrm{d}z. \tag{27}$$

For surface and uniform volume carrier generation, corresponding to (21) and (23), the constant $c = 1/2$ and $1/6$, respectively.

As follows from equation (9), the function $\Phi(t)$ decreases monotonically with time. Therefore, equations (25) and (26) describe the initial and the final parts of the TSC curve. One can show that the current $I(t)$, given by (25) and (26), is an increasing and decreasing function of time, respectively, if the function $C_t(\varepsilon, t) N_t(\varepsilon)$ slowly falls with energy. The approximate position of the TSC maximum can be found by equating these formulae, which results in the implicit equation

$$\tau_0 \Phi(\tau_e) = c^{-1/2}. \tag{28}$$

The time τ_e corresponds to the effective transit time of the carrier packet across the sample [10]. Equations (25) and (26) are respectively valid for $t \ll \tau_e$ and $t \gg \tau_e$.

Now we shall derive formulae determining the initial rise and the final decay of TSC for the general case of temperature-dependent $\mu(t)$, $C_t(\varepsilon, t)$ and $\nu(\varepsilon, t)$. Let us consider first the initial stage of carrier transport, for which carrier neutralization at the collecting

electrode is negligible, and almost all generated carriers remain in the sample. Integrating both sides of equation (12) with respect to z, and assuming that $n(z, t) \ll n_t(z, t)$, we obtain

$$\int_0^{\tau_0} n(z, t)\,dz \simeq \frac{n_0\tau_0}{w(t)}\frac{d}{dt}\left(\frac{1}{\Phi(t)}\right).$$

According to equation (5), the initial TSC rise is expressed by

$$I(t) \simeq I_0\frac{u(t)}{w(t)}\frac{d}{dt}\left(\frac{1}{\Phi(t)}\right). \tag{29}$$

Let us consider now the final stage of carrier transport, assuming that all the carriers emitted from traps of depth $\varepsilon_0(t)$ are collected at the electrode without retrapping in the energy region $\varepsilon \geqslant \varepsilon_0(t)$. The first term on the RHS of equation (13) can then be dropped, which results in

$$\frac{\partial n_t(z, t)}{\partial t} \simeq \frac{1}{\Phi(t)}\frac{d\Phi(t)}{dt}n_t(z, t).$$

Integrating this equation and making use of equations (14) and (15) yields

$$n_t(z, t) \propto \Phi(t) \qquad n(z, t) \propto -[1/u(t)]\,d\Phi(t)/dt.$$

In the above relationships, the omitted factors depend solely on z. Hence, as results from equation (5), the final TSC decay is given by

$$I(t) \propto -d\Phi(t)/dt. \tag{30}$$

Formulae (29) and (30) generalize expressions (25) and (26). In (30), however, neither the value of the proportionality constant nor its dependence on τ_0 can be determined.

3.2. Discussion

For the purposes of both the following discussion as well as the numerical calculations, we shall specify here the form of the functions $T(t)$, $\mu(t)$, $C_t(\varepsilon, t)$, $\nu(\varepsilon, t)$ and $N_t(\varepsilon)$. We assume the linear scheme of sample heating,

$$T(t) = T_0 + \beta t \tag{31}$$

where β is the heating rate. In what follows, all the quantities will be expressed in terms of sample temperature instead of time.

Except for the final part of the section, we shall neglect the energy dependences of the carrier capture coefficient and the frequency factor. This assumption is commonly used in the theory of isothermal dispersive transport and corresponds to the case of strongly coupled electron–multiphonon interactions. For weak electron–multiphonon coupling both quantities vary exponentially with energy [15, 16],

$$C_{t0}(\varepsilon) = C_{t0}(0)\exp(-\varepsilon/kT_p) \tag{32}$$

$$\nu_0(\varepsilon) = \nu_0(0)\exp(-\varepsilon/kT_p) \tag{33}$$

where the characteristic temperature T_p is related to the mean phonon energy. We

consider the usual case of the power-law dependences of $\mu(T)$, $C_t(T)$ and $\nu(T)$ on temperature (cf. I, section 3.2), corresponding to the equations:

$$u(T) = (T/T_0)^a \tag{34}$$

$$w(T) = (T/T_0)^{1/2-b}. \tag{35}$$

The value of the parameter a depends on the free-carrier scattering mechanism ($a = -3/2$ and $3/2$ for scattering on acoustic phonons and charged impurities, respectively). The value of b is determined by the kind of trapping centres ($b = 0$ and 2 for neutral and coulombic ones).

Once the sample heating mode and the form of the function $\nu(\varepsilon, T)$ are given, equation (10) determining the demarcation energy $\varepsilon_0(T)$ may be solved approximately (see appendix 2). In the present case the demarcation level is a linear function of temperature:

$$\varepsilon_0(T) = k(c^*T - T^*) \tag{36}$$

$$c^* = c_1 \ln(\nu_0/\beta T_0^{2-b}) + c_2. \tag{37}$$

The numerical values of T^*, c_1 and c_2 depend on the parameter b.

As the model trap distributions leading to dispersive transport, we choose the exponential distribution

$$N_t(\varepsilon) = (N_{tot}/kT_c)\exp[-(\varepsilon - \varepsilon_t^0)/kT_c] \tag{38}$$

and the special case of Gaussian distribution

$$N_t(\varepsilon) = (2N_{tot}/\pi^{1/2}kT_c)\exp\{-[(\varepsilon - \varepsilon_t^0)/kT_c]^2\}. \tag{39}$$

In both formulae N_{tot} stands for the total density of traps, the characteristic temperature T_c determines the rate of trap density decrease with energy and the upper limit of the trap distribution $\varepsilon_t = \infty$.

Making use of the equations obtained in the previous sections, one can now calculate the TSC for a given trap distribution. Below, only some formulae referring to the exponential one (38) are given, because of the unique features of the resulting TSC. With the neglect of the temperature dependence of $\mu(T)$ and $C_t(T)$, from equations (25), (26) and (28) one gets formulae determining the initial rise and the final drop of the TSC, as well as the temperature $T_e = T(\tau_e)$ corresponding approximately to the TSC maximum:

$$I(T) \propto \exp(\pm c^*T/T_c) \tag{40}$$

$$T_e \simeq (1/c^*)[\varepsilon_t^0/k + T^* + T_c \ln(c^{1/2}\tau_0/\tau_{t0})]. \tag{41}$$

In equation (40) the plus and minus signs refer to the temperature regions $T < T_e$ and $T > T_e$, respectively. Essentially the same formulae were derived earlier in [7, 8, 11] for the case of surface carrier generation.

From equation (41) it appears that the TSC maximum shifts towards higher temperatures with the increase of the heating rate β as well as the ratio d/E. The last dependence is a general feature of the 'TSC transport peak'. Equation (40) shows that the rates of initial rise and final decrease of the TSC are independent of the electric field and the sample thickness. On a semilogarithmic plot of $\ln I$ versus T, they are represented by straight lines of slopes $\pm c^*/T_c$. This is analogous to the 'universality' property of isothermal dispersive current transients, valid for the exponential trap distribution (see e.g. [5]). The plot of $\ln I$ versus T in the case of TSC can be viewed as the analogue of the

Scher–Montroll [1] plot of $\log I$ versus $\log t$, referring to isothermal dispersive transport. If the temperature variation of $\mu(T)$ and $C_t(T)$ is taken into account, the considered plot of TSC is not strictly linear for $T < T_e$ (compare (25) and (29)). Then, the 'universality' of the shape of TSC curves with respect to d/E does not hold rigorously.

From now on we shall consider some techniques for determining the energetic trap distribution from the TSC data. Analogous methods were proposed earlier in [10] for the case of surface carrier generation. One of them consists of fitting the temperature dependence of the charge $Q(T)$ collected in the temperature region from T_0 to T. The corresponding formula is obtained by integrating equation (20):

$$Q(T) = \frac{Q_0}{\tau_0 \Phi(t)} \left(1 - \frac{1}{n_0 \tau_0} \int_0^{\tau_0} n(z, 0) \exp[-(\tau_0 - z)\Phi(T)]\, dz\right) \tag{42}$$

where $Q_0 = I_0 \tau_0$ is the total charge generated in the sample. One can find the relationship between Q_0 and the total charge Q_∞ flowing in the measuring circuit, which corresponds to the area under the TSC curve. Since $\tau_0 \Phi(T) \ll 1$ for $T > T_e$, from equation (42) one gets

$$Q_\infty = \frac{Q_0}{n_0 \tau_0} \int_0^{\tau_0} (1 - z/\tau_0) n(z, 0)\, dz. \tag{43}$$

In the cases of surface and uniform bulk carrier generation (cf. equations (21) and (23)), $Q_\infty = Q_0$ and $Q_0/2$, respectively. Once the initial distribution of carriers is specified, from (42) and (43) one gets the formula expressing the ratio $Q(T)/Q_\infty$ in terms of the function $\tau_0 \Phi(T)$. Thus the function $\Phi(T)/\mu_0$, being proportional to the total trap density in the energy region $\varepsilon \geqslant \varepsilon_0(T)$ (cf. equation (11)), can be determined. The above procedure was applied in [17] to the reinterpretation of the TSC measurements in polyvinylcarbazole [18]. The same function may be found in the simplest way from the initial TSC increase since, as results from equation (42),

$$Q(T) \simeq Q_0/\tau_0 \Phi(T) \qquad T < T_e \tag{44}$$

or from the dependence of temperature T_e on the ratio d/E (see equation (28)). Finally, the shape of the trap distribution can be obtained directly from the final TSC decay. It follows from equation (30), as well as equations (11) and (36), that

$$I(T) \propto \beta c^* C_{t0} N_t(\varepsilon_0(T)) \qquad T > T_e. \tag{45}$$

This is in principle the formula derived by Simmons *et al* [19] under the assumption of no carrier retrapping over the whole TSC run. It should be stressed that the previous methods ignore the temperature dependence of $\mu(T)$ and $C_t(T)$, which limit their accuracy, while the last method is free from this disadvantage.

The described techniques make it possible to find the shape of the function $N_t(\varepsilon_0(T))$. Additionally, one needs to determine the position of the demarcation level $\varepsilon_0(T)$ in the energy gap as a function of temperature. We assume first that the temperature dependence of $\mu(T)$ and $C_t(T)$ has no significant influence on the shape of TSC curves. It is apparent from equation (11) that the function $\Phi(T)$ depends on the temperature only via $\varepsilon_0(T)$. Taking into account the form of equations (20), (42), (36) and (37) one can conclude that the courses of $I(T)/c^*\beta$ and $Q(T)$ for different values of β, plotted versus $c^*T - T^*$, should coincide. Thus, measurements of the TSC or the collected charge for several heating rates allow us to determine the parameters in (36) and (37) and the function $\varepsilon_0(T)$, irrespective of the kind of trapping centres. If the TSC peaks are

significantly affected by the temperature dependence of $\mu(T)$ and $C_t(T)$, the plots of $I(T)/c^*\beta$ versus $c^*T - T^*$ should overlap solely in the high-temperature region $T > T_e$ (cf. equation (30) or (45)). For this reason, it would be desirable to determine the function $\varepsilon_0(T)$ from the final TSC decay. According to equations (29) and (34)–(37) the course of $I(T)T^{1/2-a-b}/c^*\beta$ in the low-temperature region $T < T_e$, plotted versus $c^*T - T^*$, should also not depend on β. In principle, this allows one to determine the sum of the parameters a and b, which govern respectively the temperature dependence of $\mu(T)$ as well as of $C_t(T)$ and $\nu(T)$. If the temperature dependence of the microscopic carrier mobility is known *a priori*, one can calculate the value of b, which gives some information about the trapping centres, and of the frequency factor ν_0.

Let us discuss in brief the case of weak electron–phonon coupling, when $C_{t0}(\varepsilon)$ and $\nu_0(\varepsilon)$ vary exponentially with energy (see equations (32) and (33)). It is obvious that formulae (20), (29) and (30), determining TSC, as well as the majority of the resulting equations still remain valid. One should bear in mind that the integrand in equation (11) for the function $\Phi(T)$ contains in the general case $C_{t0}(\varepsilon)$ instead of C_{t0}, and that the demarcation energy $\varepsilon_0(T)$ is a non-linear function of the temperature (appendix 2). In particular, equation (45) should be replaced by

$$I(T) \propto \beta[\mathrm{d}\varepsilon_0(T)/\mathrm{d}T]\, C_{t0}(\varepsilon_0(T))N_t(\varepsilon_0(T)). \tag{46}$$

Because of another form of the expression for $\varepsilon_0(T)$, the TSC dependence on heating rate β should differ from that established before, though the discrepancy may not be very significant (cf. next section). Thus the TSC measurements for several values of β enable us in principle to distinguish between the cases of strong and weak electron–phonon coupling. In the last case, this would allow determination of the characteristic temperature T_p, the function $\varepsilon_0(T)$ and in consequence the form of the energetic trap profile.

Considering the reliability of the described techniques, one should recognize that the rate of TSC decay for $T \gg T_e$ is independent of the spatial trap distribution [20, 21], the extent of trap occupancy [22] and, probably, on the space-charge field due to generated or permanently trapped carriers. All the mentioned factors would affect the shape of the TSC peaks in the temperature region $T \leqslant T_e$ as well as their position. Therefore, the analysis of the final TSC decay utilizing formulae (45) or (46) seems to be most appropriate. It is worth noting that a similar method of determining the trap distribution from the current transient $I(t)$ for $t \gg \tau_e$ was developed in the case of isothermal dispersive transport (e.g. [23]). On the other hand, the determination of the parameters b and ν_0 from the initial rise of the TSC, as described above, may involve a significant error.

4. Numerical analysis

4.1. Monte Carlo method

In order to verify the accuracy of the formulae determining TSC, we carried out Monte Carlo simulations of non-isothermal dispersive transport. The calculation procedure is analogous to that described in I. The transport of the individual carrier is characterized by the following random variables: the free-carrier lifetime Δt_{tr}, the trap depth ε and

the carrier dwell-time Δt_r in the trap. The values of these variables are calculated repeatedly from the equations

$$\Delta t_{tr} = -\tau_t(t_{tr}) \ln(X') \tag{47}$$

$$\varepsilon = \varepsilon_t^0 - kT_c \ln(X'') \tag{48a}$$

$$\varepsilon = \varepsilon_t^0 + kT_c[-\ln(X'')]^{1/2} \sin(\pi X''') \tag{48b}$$

$$\varepsilon = \varepsilon_t^0 - [k\,T_p T_c/(T_p + T_c)] \ln(X'') \tag{48c}$$

$$\int_{t_r}^{t_r+\Delta t_r} \frac{dt}{\tau_r(\varepsilon, t)} = -\ln(X''''). \tag{49}$$

Here t_{tr} and t_r denote the moments of carrier release from the trap and of carrier capture, respectively, and $X'; \ldots, X''''$ are random numbers, uniformly distributed in the interval $(0, 1)$. Equations (48*a*) and (48*b*) concern the cases of exponential (38) and Gaussian (39) trap distributions, respectively, as well as of $C_{t0}(\varepsilon) = \text{const}$, while equation (48*c*) corresponds to the case of exponential distribution of traps (38) and $C_{t0}(\varepsilon) \propto \exp(-\varepsilon/kT_p)$. Formula (48*a*) follows from equation (47) of I and formula (48*c*) is obtained in a similar manner. Formula (48*b*) results from the Box–Muller algorithm for generating random variables of a Gaussian distribution [24]. Implicit equation (49) for Δt_r is solved numerically in a similar way as in I. The TSC curve is obtained by repeating the above procedure for a large number N of carriers and averaging the resulting current.

In all the calculations, the limit ε_t^0 of the trap distribution is set considerably greater than kT_0. The 'cut-off' in the trap density is introduced solely for calculational convenience. First, the number of 'inefficient' trapping events in the energy interval $\varepsilon < \varepsilon_0(T_0)$ is reduced. Secondly, the convergence of the series in the procedure for solving equation (49) (cf. I, appendix 3) is ameliored. From approximate equation (11), determining the function $\Phi(T)$, it is seen that its course and, in consequence, the TSC do not depend on the density of traps with depth $\varepsilon < \varepsilon_0(T_0)$ if $\varepsilon_t^0 < \varepsilon_0(T_0)$. Then, the position of the trap limit ε_t^0 in the energy gap has no essential importance.

4.2. Comparison of analytical and numerical results

In the figures, the results of Monte Carlo simulations (marked by points) are compared with those following from the approximate solutions of transport equations (shown by full and broken curves). Figures 1–4 concern the energy- and temperature-independent carrier capture coefficient and frequency factor, as well as the free-carrier mobility independent of temperature.

Figure 1 shows the TSC peaks obtained for the exponential distribution of traps (38), and both surface and uniform bulk carrier generation. The full curves are calculated from equations (22) and (24); the broken lines, which represent the initial rise and the final decay of TSC, are calculated from equations (25), (26) and (27). The function $\Phi(T)$ is computed using approximate equations (11), (36) and (A2.6), (A2.7). It is seen that the accuracy of the equations improves—as expected (cf. section 2.2)—with the increase of characteristic temperature T_c, and is rather satisfactory for the ratio $T_c/T_0 \approx 5$ (figure 1(*a*)). The semilogarithmic plot somewhat masks the discrepancies between analytical and numerical results. For example, the differences in the height of TSC peaks range from about 2% (figure 1(*a*), curve 1) to about 8% (figure 1(*b*), curve 2). In the high-temperature region the Monte Carlo results exhibit appreciable fluctuations, probably

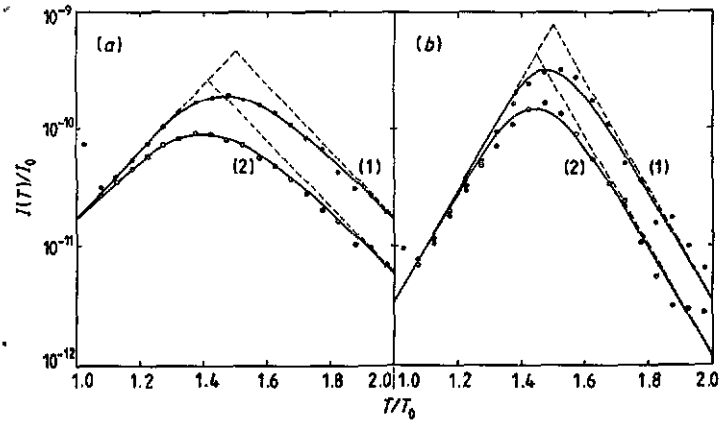

Figure 1. TSC curves calculated for exponential distribution of traps and both surface (1) and volume (2) carrier generation: $\tau_0\beta/T_0 = 10^{-10}$; $\tau_{00}\beta/T_0 = 2.28 \times 10^{-12}$ (a), 2.31×10^{-13} (b); $\nu_0 T_0/\beta = 10^{15}$; $T_c/T_0 = 5$ (a), 3 (b); $\varepsilon_t^0/kT_0 = 30$; $T_0 = 100$ K; $N = 10^4$ (a), 10^3 (b).

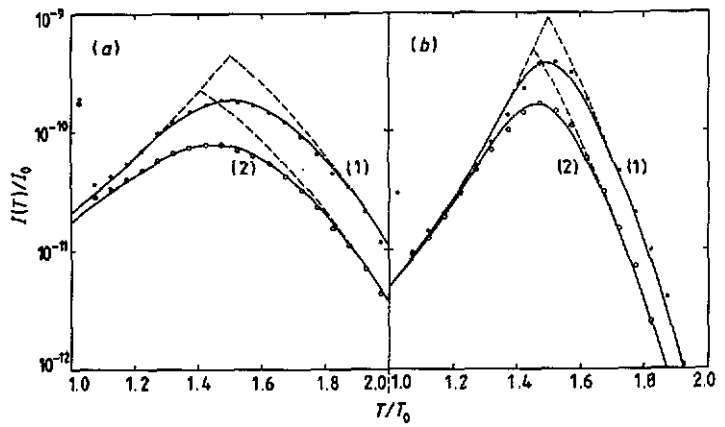

Figure 2. TSC curves obtained for Gaussian trap distribution and both surface (1) and volume (2) generation of carriers: $\tau_0\beta/T_0 = 10^{-10}$; $\tau_{00}\beta/T_0 = 7.46 \times 10^{-12}$ (a), 1.08×10^{-12} (b); $\nu_0 T_0/\beta = 10^{15}$; $T_c/T_0 = 15$ (a), 10 (b); $\varepsilon_t^0/kT_0 = 30$; $T_0 = 100$ K; $N = 2 \times 10^4$ $(a, 1)$, 4×10^4 $(a, 2)$, 4×10^3 $(b, 1)$, 8×10^3 $(b, 2)$.

due to the small number of carriers remaining in the sample. The general course of TSC suggests, however, a good coincidence with the analytical formulae.

Figure 2 presents analogous results for the Gaussian trap distribution (39). The accuracy of the approximate equations, determining TSC, again ameliorates with increasing value of T_c. In contrast to the case of the exponential distribution, the TSC peaks are asymmetric, their low-temperature half-widths being larger than the high-temperature ones. The TSC characteristics are, therefore, quite sensitive to changes in the energetic trap distribution. This proves the potential usefulness of the considered TSC method.

The plots in figures 3 and 4 correspond to identical conditions (exponential trap distribution, surface carrier generation) and data set used as curve (1) in figure 1(a). In figure 3, the time evolution of the total carrier density in the sample,

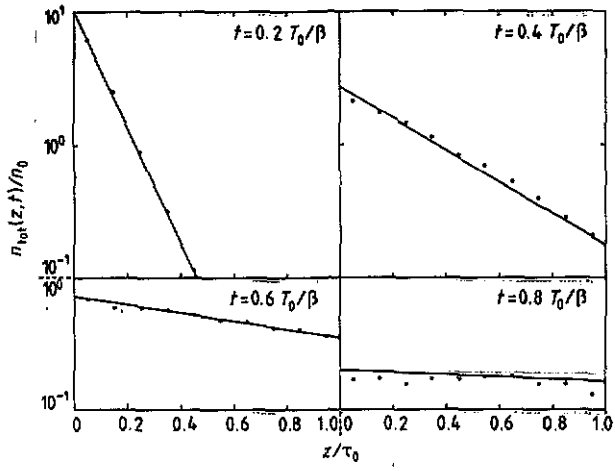

Figure 3. Spatial distribution of carriers at several times calculated for exponential trap distribution and surface carrier generation. The parameters are as in figure 1(*a*).

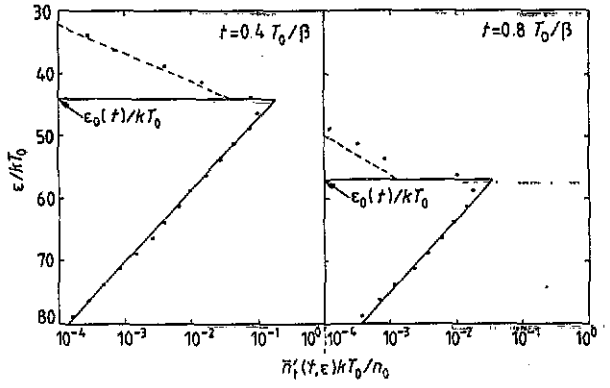

Figure 4. Energy distribution of trapped carriers averaged over sample thickness for two different times. The results are obtained for exponential distribution of traps and carrier generation at the sample surface. The parameters are as in figure 1(*a*).

$$n_{\mathrm{tot}}(z,t) = n(z,t) + n_{\mathrm{t}}(z,t)$$

is displayed. The trapped-carrier density exceeds in the present case the free one by more than nine orders of magnitude, and $n_{\mathrm{tot}}(z,t) \simeq n_{\mathrm{t}}(z,t)$. From equations (19) and (21) it follows that the trapped-carrier density should decrease exponentially with space coordinate. The numerical simulation approximately confirms this behaviour.

In figure 4, the time variation of the energetic distribution of trapped carriers $n'_{\mathrm{t}}(z,t,\varepsilon)$ is presented as its average over the sample thickness. The corresponding formulae are derived in appendix 3. The broken and full sloping lines are for the cases of thermal equilibrium between free and trapped carriers ($\varepsilon < \varepsilon_0(t)$, equation (A3.3)) and of no carrier emission from the traps ($\varepsilon > \varepsilon_0(t)$, equation (A3.5)), respectively. One should recall that equation (12), governing the carrier trapping/detrapping kinetics, was derived under the assumption of a dominant number of carriers captured in the energy

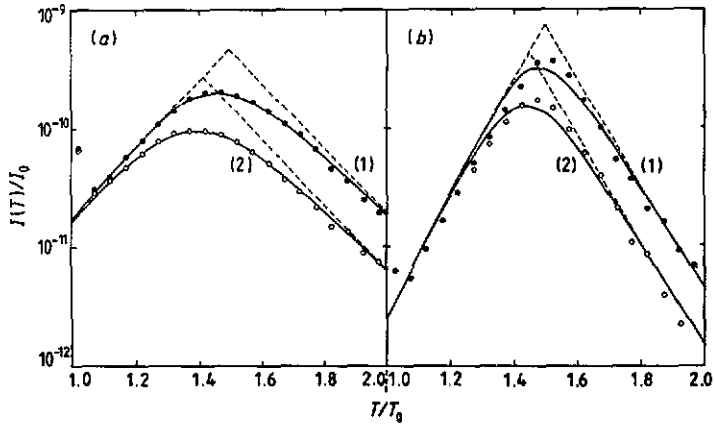

Figure 5. TSC peaks calculated for exponential trap distribution and both surface (1) and volume (2) carrier generation in the case of weak electron–phonon coupling: $\tau_0\beta/T_0 = 10^{-10}$; $\tau_{t0}\beta/T_0 = 1.87 \times 10^{-12}$ (*a*), 1.32×10^{-13} (*b*); $\nu_0(\varepsilon_t^0)T_0/\beta = 10^{15}$; $T_c/T_0 = T_p/T_0 = 8$ (*a*), 4 (*b*); $\varepsilon_t^0/kT_0 = 30$; $T_0 = 100$ K; $N = 10^4$ (*a*, 1), 2×10^4 (*a*, 2), 2.5×10^3 (*b*, 1), 5×10^3 (*b*, 2).

region $\varepsilon > \varepsilon_0(t)$. In general, the analytical formulae reproduce the numerical calculations quite well. The given results verify the concept of demarcation energy $\varepsilon_0(t)$, if only the trap density varies slowly with energy.

Figure 5 shows the TSC peaks obtained for an exponential distribution of traps with $C_{t0}(\varepsilon)$ and $\nu_0(\varepsilon) \propto \exp(-\varepsilon/kT_p)$ (weak electron–multiphonon coupling). The temperature dependence of $\mu(T)$, $C_t(\varepsilon, T)$ and $\nu(\varepsilon, T)$ is still ignored. The notations are the same as in figures 1 and 2. The function $\Phi(T)$ in equations (22) and (24)–(26) for TSC is computed from (11), (A2.6), (A2.7) and (A2.15). The accuracy of the equations should now depend mainly on the parameter T_e, defined by $T_e^{-1} = T_c^{-1} + T_p^{-1}$ which characterizes the rate of decrease of the function $C_{t0}(\varepsilon)N_t(\varepsilon)$. For $T_e = 4T_0$ (figure 5(*a*)) the accuracy is quite good, though slight deviations seem to exist in the high-temperature region. The TSC peaks have almost identical shape as those in figure 1, concerning energy-independent $C_{t0}(\varepsilon)$ and $\nu_0(\varepsilon)$ (strong electron–multiphonon coupling). This indicates that the demarcation level $\varepsilon_0(T)$, although given by non-linear expression (A2.15), shifts nearly linearly with temperature. The TSC dependence on heating rate β should then have a similar form to that corresponding to $\nu_0(\varepsilon) = \text{const}$. Thus, in experimental practice it may be difficult to discriminate between the cases of strong and weak electron–phonon coupling.

Finally, figure 6 illustrates the influence of temperature variation of $\mu(T)$, $C_t(T)$ and $\nu(T)$ on the TSC course. Figures 6(*a*) and (*b*) relate to the neutral and coulombic trapping centres, respectively; curves (1) and (2) relate to carrier scattering on acoustic phonons and charged impurities. The TSC peaks are calculated with the same assumptions (exponential distribution of traps, carrier generation at the sample surface, energy-independent $C_{t0}(\varepsilon)$ and $\nu_0(\varepsilon)$), and for identical values of the parameters at $T = T_0$ as the peaks (1) in figure 1(*b*). The initial rise and the final decrease of TSC (full lines) are computed from equations (29) and (30). The values of the unknown proportionality constant in (30) are chosen to obtain the best fit with Monte Carlo results. The accuracy of the equations is essentially the same as in figure 1(*b*). Inspection of figures 1(*b*) and 6 shows meaningful differences between the individual TSC peaks, mainly due to the

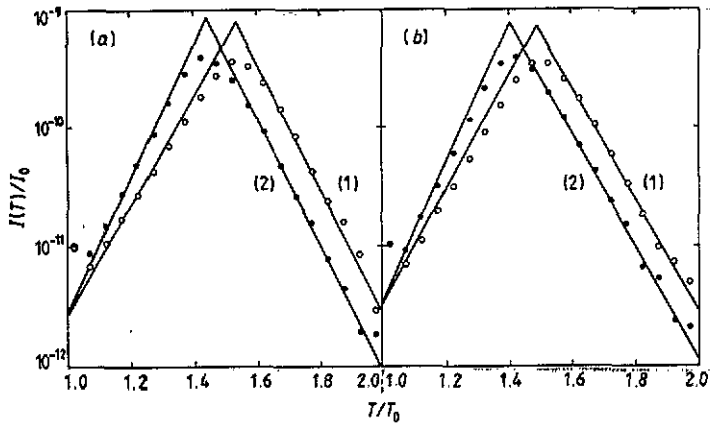

Figure 6. TSC peaks obtained for exponential distribution of traps and carrier generation at the sample surface. The individual peaks correspond to different temperature dependences of $\mu(T)$, $C_t(T)$ and $\nu(T)$. Parameters: $\tau_0\beta/T_0 = 10^{-10}$; $\tau_{t0}\beta/T_0 = 2.31 \times 10^{-13}$; $\nu_0 T_0/\beta = 10^{15}$; $T_c/T_0 = 3$; $\varepsilon_t^0/kT_0 = 30$; $T_0 = 100$ K; $a = -1.5(1), 1.5(2)$; $b = 0(a), 2(b)$; $N = 6 \times 10^3$ (1), 10^4 (2).

temperature variation of free-carrier mobility. One can conclude that the neglect of the dependence of $\mu(T)$, $C_t(T)$ and $\nu(T)$ on temperature may introduce appreciable error in the energetic trap profile, determined from the TSC data.

5. Conclusions

In this work we have investigated the TSC related to multiple-trapping dispersive carrier transport. The derived formulae have been verified by the Monte Carlo evaluation of TSC. The main attention has been paid to the case of energy-independent carrier capture coefficient and frequency factor (strong electron–multiphonon coupling). As regards this case, the following conclusions can be made.

(i) The shape of the TSC peak is determined mainly by the forms of energetic trap distribution and spatial distribution of generated carriers. The TSC is also influenced by the temperature dependence of carrier capture coefficient and frequency factor (i.e. by the kind of trapping centres) as well as of free-carrier mobility.

(ii) In principle, several techniques could be applied to the TSC data analysis. The majority of them, however, do not take into account the temperature dependence of the quantities mentioned above, and may introduce some errors into the determined energetic profiles of traps. The only exception is the method utilizing the final TSC decay.

(iii) Some information about the kind of trapping centres can be inferred from the initial increase of TSC. For this purpose, the temperature dependence of microscopic carrier mobility must be known *a priori*.

These conclusions do not change essentially when the carrier capture coefficient and the frequency factor decrease exponentially with energy (weak electron–multiphonon coupling). The TSC course is then related to the form of 'effective density' (i.e. product of density and carrier capture coefficient) of traps. In principle the cases of strong and

weak electron–phonon coupling may be distinguished on the basis of the TSC dependence on heating rate.

The TSC peaks of a similar form can also be due to hopping carrier transport between the localized states [9]. At the present stage of the theory one cannot establish the distinguishing features of TSC related to multiple-trapping and hopping transport.

The given treatment of TSC applies to strongly dispersive transport, when the trap density and the carrier capture coefficient vary slowly with energy, and the energetic distribution of trapped carriers differs significantly from the equilibrium one. There exists the possibility of an alternative approach for both isothermal and non-isothermal dispersive transport, assuming nearly perfect thermalization of captured carriers. This will be the subject of a forthcoming paper.

Acknowledgments

The author is thankful to Professor B Jachym for stimulating discussions. Dr J Rybicki's assistance in the numerical calculations and improving of the manuscript is sincerely appreciated.

Appendix 1. Solutions of equations (1)–(3) in the case of no carrier detrapping

Neglecting in equations (1)–(3) the carrier detrapping and the time dependence of $\mu(t)$ and $C_t(\varepsilon, t)$, i.e. setting $u(t) = 1$ and $\Phi(t, t') = 1/\tau_{t0}$ (cf. section 2.2), we get

$$\partial[n(z, t) + n_t(z, t)]/\partial t + \partial n(z, t)/\partial z \simeq 0 \tag{A1.1}$$

$$n_t(z, t) \simeq \frac{1}{\tau_{t0}} \int_0^t n(z, t')\, dt'. \tag{A1.2}$$

Differentiation of (A1.2) with respect to time and insertion into (A1.1) yields

$$\partial n(z, t)/\partial t + \partial n(z, t)/\partial z \simeq -n(z, t)/\tau_{t0}. \tag{A1.3}$$

The solutions of equations (A1.2) and (A1.3), corresponding to instantaneous surface carrier generation, are well known from the theory of the TOF method (see e.g. [25]). However, we need a more general solution, valid for an arbitrary initial distribution $n(z, 0)$ of generated carriers. The general solution of (A1.3), fulfilling the boundary condition (15), has the form

$$n(z, t) = n(z - t, 0) \exp(-t/\tau_{t0}) H(z - t) \tag{A1.4}$$

where $H(\ldots)$ is the unit step function. Substituting (A1.4) into (A1.2) and introducing the new integration variable $z' = z - t$ we obtain

$$n_t(z, t) = \frac{1}{\tau_{t0}} \int_{z-t}^{z} n(z', 0) \exp[-(z - z')/\tau_{t0}] H(z')\, dz'. \tag{A1.5}$$

If $t > z$, from (A1.4) and (A1.5) one gets equations (16) and (17).

Appendix 2. Expressions for demarcation energy $\varepsilon_0(T)$

We shall assume here the linear heating scheme (31) and express $\nu(\varepsilon, T)$ in the factorized form (7). Equation (10), which determines the demarcation level $\varepsilon_0(T)$, can then be written, using equations (4) and (35), as

$$\frac{\nu_0(\varepsilon_0)}{\beta}\int_{T_0}^{T}\left(\frac{T'}{T_0}\right)^{2-b}\exp\left(-\frac{\varepsilon_0}{kT'}\right)\mathrm{d}T' = 1 \tag{A2.1}$$

or, after a change of integration variable, $s = \varepsilon_0/kT'$, as

$$\frac{\nu_0(\varepsilon_0)\varepsilon_0^{3-b}}{\beta k T_0^{2-b}}\int_{\varepsilon_0/kT}^{\varepsilon_0/kT_0}\frac{\exp(-s)}{s^{4-b}}\,\mathrm{d}s = 1. \tag{A2.2}$$

If ε_0/kT, $\varepsilon_0/kT_0 \gg 1$ and T is not too close to T_0, the upper integration limit in (A2.2) may be replaced by infinity and the asymptotic formula

$$\int_{\varepsilon_0/kT}^{\infty}\frac{\exp(-s)}{s^{4-b}}\,\mathrm{d}s \simeq \left(\frac{kT}{\varepsilon_0}\right)^{4-b}\exp\left(-\frac{\varepsilon_0}{kT}\right) \tag{A2.3}$$

may be used (cf. I, equations (A2.4) and (A2.5)). Thus, from (A2.2) and (A2.3) one gets the equation

$$\exp(\varepsilon_0/kT) \simeq \nu_0(\varepsilon_0)kT^{4-b}/\beta T_0^{2-b}\varepsilon_0. \tag{A2.4}$$

Let us consider first the case of strong electron–phonon coupling, $\nu_0(\varepsilon) = \text{const}$, and rewrite equation (A2.4) in the form

$$\varepsilon_0/kT \simeq \ln(\nu_0 kT^{4-b}/\beta T_0^{2-b}\varepsilon_0). \tag{A2.5}$$

Since $\nu_0 T_0/\beta \gg 1$, the RHS of (A2.5) is a slowly varying function of ε_0 and T. Therefore, $\varepsilon_0(T)$ may be well approximated by a linear function (36) of temperature. The values of coefficients in (36) and (37) can be determined by solving numerically equation (A2.5) for some range of T and $\nu_0/\beta T_0^{2-b}$. For coulombic ($b = 2$) and neutral ($b = 0$) centres one obtains, respectively,

$$c^* = 0.967\ln(\nu_0/\beta) + 3.7 \tag{A2.6}$$

$$T^* = 180\ \mathrm{K} \tag{A2.7}$$

[26] and

$$c^* = 0.974\ln(\nu_0/\beta T_0^2) + 16.6 \tag{A2.8}$$

$$T^* = 700\ \mathrm{K}. \tag{A2.9}$$

Here, ν_0/β is expressed in K^{-1} and T_0 in K. Formulae (A2.8) and (A2.9) were obtained by fitting the function $\varepsilon_0(T)$ in the temperature range $100\ \mathrm{K} \leqslant T \leqslant 450\ \mathrm{K}$ for $10^7\ \mathrm{K}^{-3} \leqslant \nu_0/\beta T_0^2 \leqslant 10^{12}\ \mathrm{K}^{-3}$. The accuracy of equation (36) is then better than 6%. The accuracy of equations (11), (36), (A2.8) and (A2.9), determining the function $\Phi(T)$ for neutral centres, is illustrated by figure A.1.

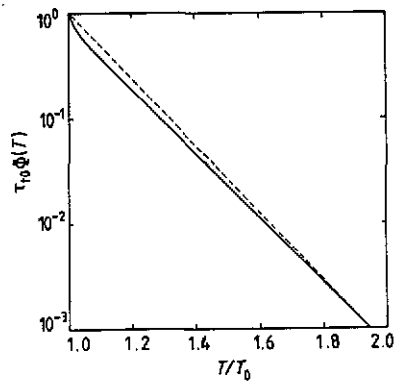

Figure A.1. Function $\Phi(T)$ for exponential trap distribution calculated from exact formula (3) (full curve) and from approximate formulae (11), (36) and (A2.8), (A2.9) (broken line): $\nu_0 T_0/\beta = 10^{15}$; $T_c/T_0 = 5$; $\varepsilon_t^0/kT_0 = 30$; $T_0 = 100$ K.

Let us consider now the case of weak electron–phonon coupling, when $\nu_0(\varepsilon)$ decreases exponentially with energy (cf. equation (33)). From equation (A2.4) one then gets

$$(\varepsilon_0/k)(1/T + 1/T_p) \simeq \ln[\nu_0(0)\, kT^{4-b}/\beta T_0^{2-b}\varepsilon_0]. \tag{A2.10}$$

This equation can be transformed to a form identical to (A2.5) by introducing the new variables $\bar{\varepsilon}_0$ and $\bar{T}$, defined by

$$\bar{\varepsilon}_0/\bar{T} = \varepsilon_0(1/T + 1/T_p) \tag{A2.11}$$

$$\bar{\varepsilon}_0/\bar{T}^{4-b} = \varepsilon_0/T^{4-b} \tag{A2.12}$$

or, explicitly, by

$$\bar{\varepsilon}_0 = \varepsilon_0(1 + T/T_p)^{(4-b)/(3-b)} \tag{A2.13}$$

$$\bar{T} = T(1 + T/T_p)^{1/(3-b)}. \tag{A2.14}$$

Hence, $\bar{\varepsilon}_0(\bar{T})$ can be approximated by a linear function of $\bar{T}$ with the same coeficients c^* and T^* as in (36) (in (A2.6) and (A2.8) ν_0 should be replaced by $\nu_0(0)$). Returning to the variables ε_0 and T with the aid of (A2.13) and (A2.14) one gets the formula

$$\varepsilon_0(T) = k[c^*T(1 + T/T_p)^{1/(3-b)} - T^*]/(1 + T/T_p)^{(4-b)/(3-b)}. \tag{A2.15}$$

The above transformation does not hold for $b = 3$, but we shall not consider this exceptional case.

Appendix 3. Energetic distribution of trapped carriers

The equation governing the kinetics of carrier trapping and detrapping for a given energy level has the form

$$\partial n_t'(z, t, \varepsilon)/\partial t = C_t(\varepsilon, t)N_t(\varepsilon)n(z, t) - n_t'(z, t, \varepsilon)/\tau_r(\varepsilon, t) \tag{A3.1}$$

(I, equation (2)), where $n_t'(z, t, \varepsilon)$ is the carrier density in the traps per unit energy. The first and second terms on the RHS are the rates of carrier capture and emission, respectively. In what follows, we assume for simplicity that $C_t(\varepsilon, t) = \text{const}$.

As indicated in section 2.2, the carriers captured in the energy range $\varepsilon < \varepsilon_0(t)$ are essentially in thermal equilibrium with the free carriers. One can then set in (A3.1) $\partial n_t'(z, t, \varepsilon)/\partial t = 0$, which gives

$$n_t'(z, t, \varepsilon) = C_t N_t(\varepsilon)\tau_r(\varepsilon, t)n(z, t) \qquad \varepsilon < \varepsilon_0(t). \tag{A3.2}$$

Averaging this expression over z one obtains

$$\overline{n_t'}(t, \varepsilon) = C_t N_t(\varepsilon)\frac{\tau_r(\varepsilon, t)}{\tau_0}\int_0^{\tau_0} n(z, t)\,\mathrm{d}z. \tag{A3.3}$$

The probability of carrier emission from the traps having depth $\varepsilon > \varepsilon_0(t)$ is very small and the second term on the RHS of (A3.1) may then be dropped. This yields

$$n_t'(z, t, \varepsilon) = C_t N_t(\varepsilon)\int_0^t n(z, t')\,\mathrm{d}t' \qquad \varepsilon > \varepsilon_0(t) \tag{A3.4}$$

and

$$\overline{n_t'}(t, \varepsilon) = \frac{C_t N_t(\varepsilon)}{\tau_0}\int_0^t \left(\int_0^{\tau_0} n(z, t')\,\mathrm{d}z\right)\mathrm{d}t'. \tag{A3.5}$$

The calculations of $\overline{n_t'}(t, \varepsilon)$ can be facilitated by recognizing that the integrals in (A3.3) and (A3.5) are proportional to $I(t)$ and $Q(t)$, respectively (cf. equations (5), (20) and (42)). Obviously, the demarcation limit between both energy regions cannot be sharp. In fact, there exists some intermediate region in the vicinity of $\varepsilon_0(t)$ in which equations (A3.3) and (A3.5) do not apply (see figure 4).

References

[1] Scher H and Montroll E W 1975 *Phys. Rev.* B **12** 2455
[2] Noolandi J 1977 *Phys. Rev.* B **16** 4466
[3] Noolandi J 1977 *Phys. Rev.* B **16** 4474
[4] Schmidlin F W 1977 *Phys. Rev.* B **16** 2362
[5] Pfister G and Scher H 1978 *Adv. Phys.* **27** 747
[6] Marshall J M 1983 *Rep. Prog. Phys.* **46** 1325
[7] Samoć M and Samoć A 1980 *Phys. Status Solidi* a **57** 667
[8] Plans J, Zieliński M and Kryszewski M 1981 *Phys. Rev.* B **23** 6557
[9] Plans J, Baltá Calleja F J, Zieliński M and Kryszewski M 1983 *Phil. Mag.* B **48** 289
[10] Tomaszewicz W and Jachym B 1984 *J. Non-Cryst. Solids* **65** 193
[11] Schrader S and Kryszewski M 1985 *Phys. Status Solidi* a **91** 243
[12] Arkhipov V I, Iovu M S, Rudenko A I and Shutov S D 1979 *Phys. Status Solidi* a **54** 67
[13] Arkhipov V I and Rudenko A I 1982 *Phil. Mag.* B **45** 189
[14] Rudenko A I and Arkhipov V I 1982 *Phil. Mag.* B **45** 209
[15] Kagawa T and Matsumoto N 1983 *J. Non-Cryst. Solids* **59–60** 477
[16] Nebel C E and Bauer G H 1989 *Phil. Mag.* B **59** 463
[17] Tomaszewicz W and Jachym B 1983 *J. Phys. D: Appl. Phys.* **16** L33
[18] Stasiak M, Jeszka J K, Zieliński M, Plans J and Kryszewski M 1980 *J. Phys. D: Appl. Phys.* **13** L221
[19] Simmons J G, Taylor G W and Tam M C 1973 *Phys. Rev.* B **7** 3714
[20] Tomaszewicz W, Rybicki J, Jachym B, Chybicki M and Feliziani S 1990 *J. Phys.: Condens. Matter* **2** 3311
[21] Rybicki J, Feliziani S, Tomaszewicz W, Jachym B and Chybicki M 1991 *J. Phys.: Condens. Matter* **3** 4229
[22] Tomaszewicz W 1992 unpublished
[23] Seynhaeve G F, Barclay R P, Adriaenssens G J and Marshall J M 1989 *Phys. Rev.* B *Condens. Matter* **39** 10196
[24] Dahlquist G and Bjorck A 1974 *Numerical Methods* (Englewood Cliffs, NJ: Prentice-Hall) ch 11
[25] Zanio K R, Akutagawa W M and Kikuchi R 1968 *J. Appl. Phys.* **39** 2818
[26] Simmons J G and Taylor G W 1972 *Phys. Rev.* B **5** 1619